Marine Pollution Bulletin 138 (2019) 193–205

Contents lists available at ScienceDirect

Marine Pollution Bulletin

journal homepage: www.elsevier.com/locate/marpolbul

Microplastic content variation in water column: The observations employing a novel sampling tool in stratified Baltic Sea

M.B. Zobkov[a,*], E.E. Esiukova[b], A.Y. Zyubin[c], I.G. Samusev[c]

[a] Northern Water Problems Institute of Karelian Research Centre of the Russian Academy of Sciences, 50 A.Nevskogo prospekt Petrozavodsk, Karelia 185030, Russia
[b] Shirshov Institute of Oceanology, Russian Academy of Sciences, 36, Nahimovskiy prospekt, Moscow 117997, Russia
[c] Immanuel Kant Baltic Federal University, 14, A. Nevskogo street, Kaliningrad 236016, Russia

ARTICLE INFO

Keywords:
Microplastic
Stratification
Vertical distribution
Bulk water sampling
The Baltic Sea
Sampling tool

ABSTRACT

A new tool was developed for microplastics (MPs) investigation in the water column. It can collect several cubic meters of water from predefined water layers down to 100 m. The tool was tested in the Baltic Sea during the period of spring thermocline formation. Strong MPs stratification was observed at all of the sampled stations. On coastal stations (~30 m deep), stratification with high fibers content was associated with the proximity of terrestrial sources and estuarine discharges, while on off-shore stations the variability of MPs was related to vertical thermohaline structure. Mean MPs content was the 32.2 (SD 50.4) pcs/m^3. Elevated MPs concentrations were observed in subsurface, near-bottom and thermohaline layers compared with intermediate layers. The heterogeneity of MPs distribution suggests that MPs particles can be retained above the density-gradient layers in coastal seas and the World Ocean.

密度梯度层

1. Introduction

Invasion of microplastics (MPs) into the marine environment is known as an emerging ecological threat (Thompson et al., 2004). It persists in different water environments: on the water surface, in bulk water and sediments over the world (Hidalgo-Ruz et al., 2012). However, to understand the MPs fate in water environment and ways of its migration, the need of quantitative and qualitative monitoring of MPs in all relevant parts of aquatic ecosystems was stated (Andrady, 2011; Hidalgo-Ruz et al., 2012; Gorokhova, 2015).

Microplastics have been identified as an open ocean pollutant since the 1970s (Carpenter and Smith, 1972) from its first observation and quantification in neuston nets with 330 μm mesh size. Subsequently, these sampling procedures were recognized as a proper way of MP content estimation and are used worldwide now (Hidalgo-Ruz et al., 2012). However, recently the amount of floating plastics has been estimated around 250,000 tons (Eriksen et al., 2014). This is at least one order of magnitude lower than plastic waste input into the marine environment, which was assessed in the range of 4.8–12.7 millions tons in 2010 only (Jambeck et al., 2015). This way, a large uncounted fraction of plastic waste potentially exists in marine environment (Enders et al., 2015). Whereas a large portion of the MP pool is definitely buried in the sediment (Woodall et al., 2014), it was shown that turbulence due to wind (Kukulka et al., 2012; Collignon et al., 2012) and storm (Lattin et al., 2004) actions can significantly affect plastic particles distribution (Kukulka et al., 2012). The size, shape and plastic density have a major effect on MPs settling velocity (Chubarenko et al., 2016; Khatmullina and Isachenko, 2017) and MPs mobility in the water column as a result. It was shown that the majority of subsurface net tows at the layers above 25 m contained plastic and it was not just surface-trapped, but was vertically distributed within the mixed layer (Kukulka et al., 2012).

船绳

The observations with Manta trawls, Bongo nets and epibenthic sled on different water levels demonstrate the same order of magnitude of MP content throughout the water column, which is slightly increased on surface and near bottom (Moore et al., 2005). Bagaev et al. (2017b) obtained the same results using Niskin bottles. Such distribution was explained with the presence of other types of vertical flows (e.g. downwelling) or the occurrence of plastics rising from deeper waters due to previous wind-driven mixing events (Reisser et al., 2015).

卡盖式采水器

So, surface tow measurements were found to significantly underestimate the total plastic content (Kukulka et al., 2012). In spite of their worldwide application (Eriksen et al., 2014; Lusher et al., 2015), surface tows were also criticized because of inaccuracy in water volume measurements and relatively coarse mesh size (Setälä et al., 2016). The last one is especially important because of the sufficient contribution of smaller size fractions to total plastic load (Desforges et al., 2014). Small MPs were found to be more abundant in the water column (Reisser

表面拖曳采样缺点众多

* Corresponding author.
E-mail address: duet@onego.ru (M.B. Zobkov).

https://doi.org/10.1016/j.marpolbul.2018.11.047
Received 17 May 2018; Received in revised form 19 November 2018; Accepted 19 November 2018

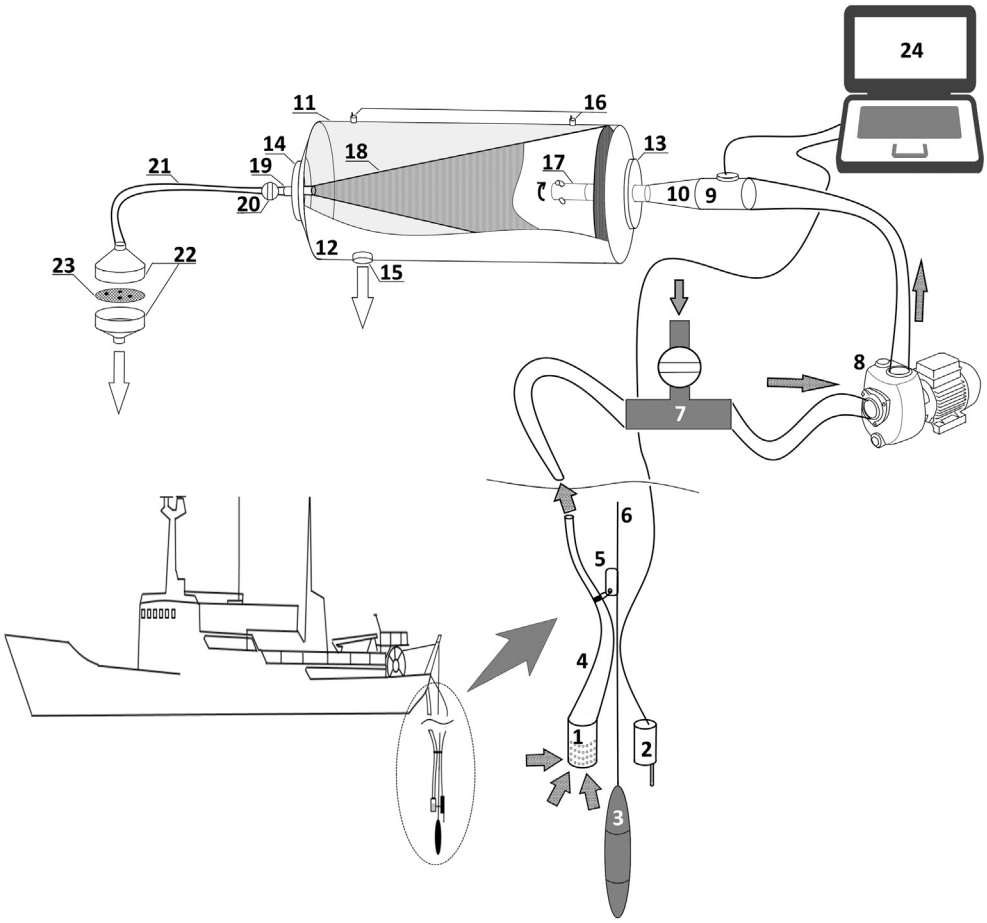

Fig. 1. The layout diagram of the PLEX.
1 – primary water intake gauze (aperture 5 mm); 2 - temperature/pressure sensor; 3 - pulling weight; 4 – inlet hose; 5- camlock clip; 6 - nylon rope with wireline ending; 7 – T-socket with ball valve for connection to vessel's seawater intake; 8 – rotary pump; 9 - flow gauge; 10 – inlet union; 11 – filtration unit; 12 – filter case; 13 – inlet flange; 14 – outlet flange; 15 – waste water outlet; 16 – vent valves; 17 – rotating spraying nozzle; 18 – filtering net; 19 – outlet union; 20 –outlet valve; 21 – outlet hose; 22 –filter holder; 23 - sampling filter; 24 – laptop computer.

et al., 2015; Cózar et al., 2014) and more susceptible to vertical transport (Reisser et al., 2015) compared with large ones. The numerical modelling suggested that incipient pycnocline is able to affect the vertical distribution of the smallest fraction of MPs (Enders et al., 2015).

The need for investigations of plastic particles throughout the water column (Thompson et al., 2004; Doyle et al., 2011), depth profiling to understand the ability of vertical MP migration with upwelling events (Desforges et al., 2014), high-resolution multi-level plastic sampling (Reisser et al., 2015) is urgent for better understanding of the vertical transport of plastics.

Different samplers were applied for MPs vertical distribution assessment. Bongo or Working Party (WP) 2 nets were applied widely by Doyle et al. (2011), Moore et al. (2005), Frias et al. (2014), Gorokhova (2015) for bulk water sampling down to 212 m, however this sampling method involved a relatively thick water layer and gave only integrated MP content. The results of episodic samplings with an Epibenthic sled (Moore et al., 2005), a messenger-operated closing trawl (Kukulka et al., 2012), a Hardy Plankton Recorder (Frias et al., 2014) are also available. However, they are underway-operated and none of them is able to maintain the sampling depth precisely, which is required to assess MPs vertical distribution induced not just by weather conditions, but also by temperature and salinity gradients. The contamination control procedures cannot be involved into the net sampling practice because of inability to control or eliminate the airborne contamination during net operation on a ship's deck (Setälä et al., 2016).

Underway sampling from subsurface water layers by using vessels seawater intake has also been independently tested recently by several researches (Desforges et al., 2014; Reisser et al., 2015; Lusher et al., 2014, 2015; Enders et al., 2015). The water pumping involving specialized submersible pumps was applied for MPs sampling by Ng and Obbard (2006), Zhao et al. (2014, 2015), Setälä et al. (2016). These methods seem to be advantageous compared with net sampling because it is possible to sample water from a defined location at different water levels, use different mesh sizes, provide precise volumetric measurements and inclusion of a routine contamination control (Setälä et al., 2016). However, they also have some limitations. They do not permit to sample from a real surface layer, and the maximum sampling depth is currently limited to several meters because of the submersible pump's water resistance rating. Thus, provided the limitation of maximum sampling depth is overcome, the pumping system can be observed as a promising way of bulk water sampling. With this regard, we designed a new sampling tool called PLEX (PLastic EXplorer).

The PLEX is based on a self-priming pump that is able to collect water from a predefined layer. The pump is deployed on a vessel's deck and does not require any specialized waterproof rating. The tool is able to collect several cubic meters of water from different layers down to 100 m and subside suspension on a single filter. It was tested in the Baltic Sea during the spring period of the thermocline formation. The Baltic Sea is known to have a heterogeneous salinity structure due to relatively large freshwater drain and accidental inflows of saline Atlantic waters (Leppäranta and Myrberg, 2009). This allowed us to assess the vertical MPs distribution in conjunction with water column thermal and salinity structure. The instrument operation concept and testing results are presented here, emphasizing the influence of a vertical density stratification on distribution of MPs concentrations in the Baltic Sea water column.

2. Materials and methods

2.1. PLEX instrument

The PLEX instrument was designed for bulk water sampling from various depths and in-line filtering of a few cubic meters of water and allows one to obtain only one small filter containing suspended matter per sample as a result. The operations with a sampling filter on a ship's deck are minimized, which allows us to decrease and control airborne contamination during sampling.

The concept of this sampling device was evolved from the work (Checkley Jr. et al., 1997), where a continuous underway fish egg sampler (CUFES) was proposed. However, our construction is more compact and deployable than the prototype and has specific arrangements for multilayer water sampling.

PLEX (Fig. 1) consists of a primary gauze (1) with a 5-mm aperture to remove larger items of debris, a sectional 2″ intake flexible hose (4) with clamp connections to deliver the water to the filtering device, a self-priming rotary pump Saer AP/97A (8) for sea water delivery and a highly efficient filtration unit (11) for suspended matter concentration with no airborne contamination. A sampling filter holder (22) with a sampling filter (23) is mounted on the outtake manifold (21) for further laboratory control. The temperature/pressure sensor (2) is mounted near the primary gauze (1) to control the sampling depth and water temperature. A flow gauge (9) is mounted between the pump and the filtration unit. The flow gauge and the temperature/pressure sensor are connected to a laptop to control sampling parameters. The instrument design allows future system extension with optical in-situ detector (FlowCam or similar) mounted between filtration unit and sampling filter. This enables in-line counting of suspended matter with capability of MPs detection.

The filtration unit (11) consists of a stainless steel case (12), a filtering net with 174 μm mesh size (18), waste water outlets (15), a rotating spraying nozzle (17) and vent valves (16) for air removal. The spraying nozzle is able to rotate freely and has two ¾″ outlets 45° angled to water flow direction. They allow the nozzle to rotate under the water flow when sampling and clean the net surface from the adherent suspended material. The rate of intake water to water passing through the filter net is about 100:1.

The self-priming rotary pump Saer AP/97A can lift water up to 8 m height. It is quite enough to sample seawater even from large research vessels, whose ship's deck elevation over the sea surface is about 4–5 m. However, our tests showed that it takes about 20 min to fill the inlet hose and pump fully before sampling and to lift the water on a ship's deck. It sufficiently delays the sampling and makes it more expensive because of the required extra shipping time. To quicken the preparing process, the pump needs to be filled externally, using the ship's seawater intake or the fire extinction system. To fill the pump and inlet hose, the filling attachment with a ball valve (7) is connected to ship's seawater intake. This allowed us to reduce preparation time at least tenfold.

2.2. Operation

Vertical position and tension of the inlet hose was maintained using a 75-kg pulling weight, which was connected to a 10-mm nylon rope. A steel wireline five meters long (6 mm in diameter) was mounted between the weight and the rope to avoid external contamination from the rope. The primary water intake gauze was mounted 0.5 m above the weight with a stainless steel carabiner. The ship's winch was applied for rope slippage and winding.

When the primary water intake gauze is set on a predefined layer with the winch, the pump is switched on and the ball valve of the filling attachment is opened. The flow gauge with the joint hose must be disconnected from the filtration unit beforehand to prevent its contamination from the seawater intake system and the water flow needs to be redirected overboard. When the flow became stable, the external water supply from the ship's seawater intake must be stopped by closing the ball valve. Then, 200 l of sea water needs to be passed through the pump, the inlet and joint hoses to wash out any possible contamination from the seawater intake system. After that, the pump should be stopped and the inlet union together with a flow gauge and flexible hose should be connected to the filtration unit. A new sampling filter must be installed into the filter holder and water sampling can be initiated by starting the pump after opening the outlet valve. After filtration of the predefined water volume (2–3 m^3), the pump must be stopped and the outlet valve needs to be closed to stop water supply to the sample filter before its extraction. The sample filter must be retrieved for further laboratory analysis. To reach the next sampling layer, the inlet hose must be disconnected from the pump and extended with another one of the required length. Several hoses can be attached one to another to reach deeper layers. The hoses are fixed to the rope with a stainless steel camlock clip every 10 m to prevent extensive hose rocking and disconnection. The foregoing operations need to be conducted on every sampling layer.

2.3. Sampling

During our test sampling, the parts of PLEX were separately deployed on a ship's deck during the passage and were assembled together every time prior to arrival to a sampling station. The water sampling began from the subsurface layer (0.5–1 m below the surface) and ended at the depth of 1–2 m above the bottom. CTD profiling was conducted on every station prior to sampling and sampling layers were planned according to the vertical temperature and salinity structure. Depending on the vertical structure, up to six sampling layers were planned:

- subsurface layer, 0.5–1 m below the surface (depending on the sea state);
- above the thermocline;
- within the cold intermediate layer (CIL);
- above the halocline;
- in the middle between the halocline and the bottom;
- bottom layer (1–2 m above the bottom).

2.4. Filters handling, contamination prevention and control

Sampling filters 50 mm in diameter with 174 μm mesh size were prepared in the laboratory and inspected under a microscope to detect possible contamination. Sampling filters were stored in preliminarily cleaned and dried glass Petri dishes which were then enveloped in paper and stored in steel boxes in a refrigerator under 4 °C until laboratory analysis. After the sampling, the filters were quickly moved from a filter holder to a Petri dish and the inner part on the filter holder was rinsed from a syringe with distilled water into the same Petri dish. The filter operation lasted no > 1 min.

Procedural blanks were prepared on each station. A clean sampling filter was placed into an opened Petri dish and rinsed with distilled water from a syringe. The filter was exposed to environmental conditions for the same duration as sampling filters. Procedural blanks were stored and processed in the same way as sampling filters.

Control samples were used to assess the numbers of MPs potentially clogged to the net surface. They were formed after sampling on each station the following way. The filtering net was removed from the filter case, connected to the filter holder with a preliminarily inserted clean sample filter and externally washed with water from the vessel's seawater intake to retrieve suspended material clogged to the internal net surface. The control filters were processed in the same way as sampling filters. To prevent external contamination of the hoses, they were connected end-to-end and bundled during storage on a ship's deck.

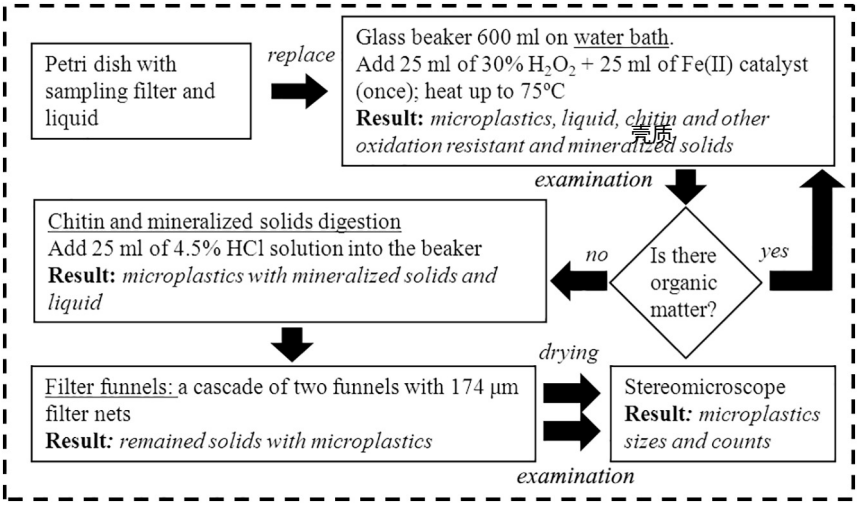

Fig. 2. Analysis procedures.

2.5. The laboratory analysis

The water samples analysis was evolved from (Masura et al., 2015) and was unified with our previous works for sediment samples processing (Zobkov and Esiukova, 2017a; Zobkov and Esiukova, 2017b). Sampling filters, procedural blanks and control samples were delivered to the laboratory in Petri dishes and processed equally. The sampling filters were carefully placed into a 600 ml glass beaker with tweezers and internal surfaces of the Petri dish were rinsed with distilled water from the syringe, draining the liquid into the beaker (Fig. 2). Multiple iterations of wet peroxide oxidation on a water bath with the Fenton's reagent (Tagg et al., 2017) were applied until all organic matter was oxidized. Digestion with HCl solution was applied to dissolve residuary chitin fractions and other mineralized solids when necessary. A sampling filter was washed with distilled water using a syringe, draining the liquid into the beaker and placed into a clean Petri dish with tweezers. The remaining solution was cooled and later filtered through the cascade of two filter funnels with preliminarily installed 174 µm filter nets (Zobkov and Esiukova, 2017a). Filter nets containing solids were rolled up, tied and placed into a clean Petri dish. They were dried at a room temperature for 24 h in slightly opened Petri dishes placed in containers covered with a sieve cloth to prevent airborne contamination.

Undissolved solids from every sample were settled on three separate filters. MPs were detected directly on the filters, which were analyzed under a stereomicroscope (Micromed MC2 Zoom Digital, magnification from 10× to 40×) in accordance with the recommendations (Norén, 2007). MPs sizes were measured only for colored MPs in their longest direction using a microscope length scale.

The extracted microplastics were classified into three groups: fragments, films, and fibers according to (Zobkov and Esiukova, 2017a). Morphological characterization of microplastics was given according to their form, color, transparency and surface structure. The chemical identification of microplastics was performed using µ-Raman spectroscopy; the most abundant types of MPs found in different stations were selected for spectroscopical analysis with reference to their morphological characteristics.

2.6. Microspectroscopical analysis

Raman spectra of the microplastic specimens were obtained using a Raman Centaur U (LTD ≪NanoScanTechnology≫, Russia) spectrometer. The spectrometer was equipped with three different interchangeable excitation sources: 632.8 nm He-Ne laser (37 mW), 532 nm, and 473 nm DPSS lasers (45 mW) which were applied when required to avoid the dyes fluorescence in colored microplastics, which was evident to be the major problem of polymer identification using micro Raman spectrometers (Zhao et al., 2007; Ghosal et al., 2018). The optical scheme of the spectrometer included an Olympus BX41 microscope (Olympus, Japan) with a 100× (NA 0.9) objective to perform beam positioning and scattered photons collection. The spectrometer monochromator had a focal length of 800 mm, 600 g/mm holographic diffraction grating and was equipped with a 1024 × 256 pixels CCD thermoelectric cooled detector (Andor Tech., UK). Microplastic specimens were put on the chemically purified quartz glass and placed in the microscope holder. The laser beam was positioned on the specimen manually using a USB Video Camera (Olympus, Japan) and the laser spot from the Raman spectrometer was focused on the specimen's surface. The size of the laser spot varied from 1 × 25 µm to 1 × 30 µm depending on the laser power used. To prevent sample destruction and achieve the best signal-to-noise ratio, the laser power embedded to the sample was manually adjusted from 5 to 37 mW for He-Ne excitation source and from 5 to 45 mW for DPPS lasers. The notch filters were applied to eliminate Rayleigh scattering. For small specimens (< 100 µm) generally made of PE, PP, cellulose acetate, carbon and nylon, the maximum available laser power with a prolonged acquisition time (120–500 s) was applied. For other specimens (≥100 µm) made of polyester, PET, PA, resins and other polymer types, especially with high fluorescent dye content, the laser power was reduced to 5–20 mW for both He-Ne and DPPS sources and CCD with a reduced acquisition time (from 5 to 60 s). The acquisition time and number of averages were selected manually to get a best signal-to-noise ratio. Raman spectra were recorded in a wavenumber ≪fingerprint≫ range for polymers between 600 cm^{-1} and 1750 cm^{-1} with the spectral resolution of 4 cm^{-1}. The instrument was calibrated before the assessment of each series of specimens with silicon standard (Horiba, Japan) at a static spectrum centered at 519.8 cm^{-1} for 1 s. All spectral data was saved after the registration as .txt files for further assessment.

A BioRad-KnowItAll Informatics System (Thermo Fisher Scientific Inc., USA) was used for manual linear baseline correction and Savitzky–Golay filtering. All spectra were normalized to the maximum signal intensity. Both KnowITAll Raman spectral libraries of plastic polymers and literature data (Araujo et al., 2018) were used for spectral identification. The identification was deemed to be successful if the hit ratio between the specimen spectra and reference spectra was above 70%.

2.7. Statistical analysis

The nonparametric Mann-Whitney *U* test was applied to determine

if there was any difference in MPs concentration between the nearby water layers. The following groups were considered: subsurface layers, thermohaline layers, intermediate layers and near the bottom layers. Subsurface and near bottom layer groups included only one corresponding sample per station each. The thermohaline layer group included all samples, collected above or inside the density gradients (thermoclines or haloclines). The intermediate layer group incorporated all samples situated between the layers mentioned above.

To test the significance in the difference between the MPs concentration in blanks and scientific samples, the Wilcoxon Signed Ranks nonparametric test was applied. Nonparametric tests were applied because the data violated the assumption of normality. Parametric Person *t*-test was run to establish if there was any relationship between the size distribution of colored MPs and the sampling depth. Log transformation was applied to normalize the data. The tests were run using the SOFA statistics software (www.sofastatistics.com). The confidence intervals (CI) of the results presented below were calculated using t-statistics with a statistical significance level $p = 0.05$.

3. Study area

Bulk water samples were collected with PLEX from 3 to 6 April 2017 at four stations in the southeastern part of the Baltic Sea within the Russian exclusive economic zone during 135 cruise of RV Professor Shtokman (Fig. 3, Table 1). At every station, from 4 to 6 horizons were sampled, see Table 1 for details. Detailed meteorological situation before and during sampling activities are given in Supplementary (Figs. S1, S2).

Two stations (**A** and **B**) were situated above the coastal slope 12 and 25 km northwest of the Strait of Baltiysk entrance. Two kilometers long, the Strait of Baltiysk links the Vistula Lagoon, the second largest shallow lagoon in the region, with the Baltic Sea. The Vistula Lagoon receives discharge of > 20 rivers including the Pregola, the Elbląg, the Pasłęka, the Nogat, etc. with a total catchment area of 23,871 km^2, the annual water exchange with the sea 20.7 km^3 and the population more than one million residents (Chubarenko, 2008; Rozynski et al., 2015).

Station **C** was situated in the head of the exclusive economic zone on a maximum distance offshore (120 km), on a rapidly plunging slope of the southern part of the Gotland Deep. Station **D** was situated 22.5 km away from the coast, above the coastal slope of the Curonian-Sambian plateau, 6.5 km away from the Lukoil's Kravtsovskoye (D6) Oil Platform.

CTD profiling was implemented on every station with hydrological complex Hydro bios MWS 12 Slimline. CTD profiling was also conducted on 17 stations in the area of the Strait of Baltyisk to establish the impact zone of freshened waters of the Vistula lagoon.

湖

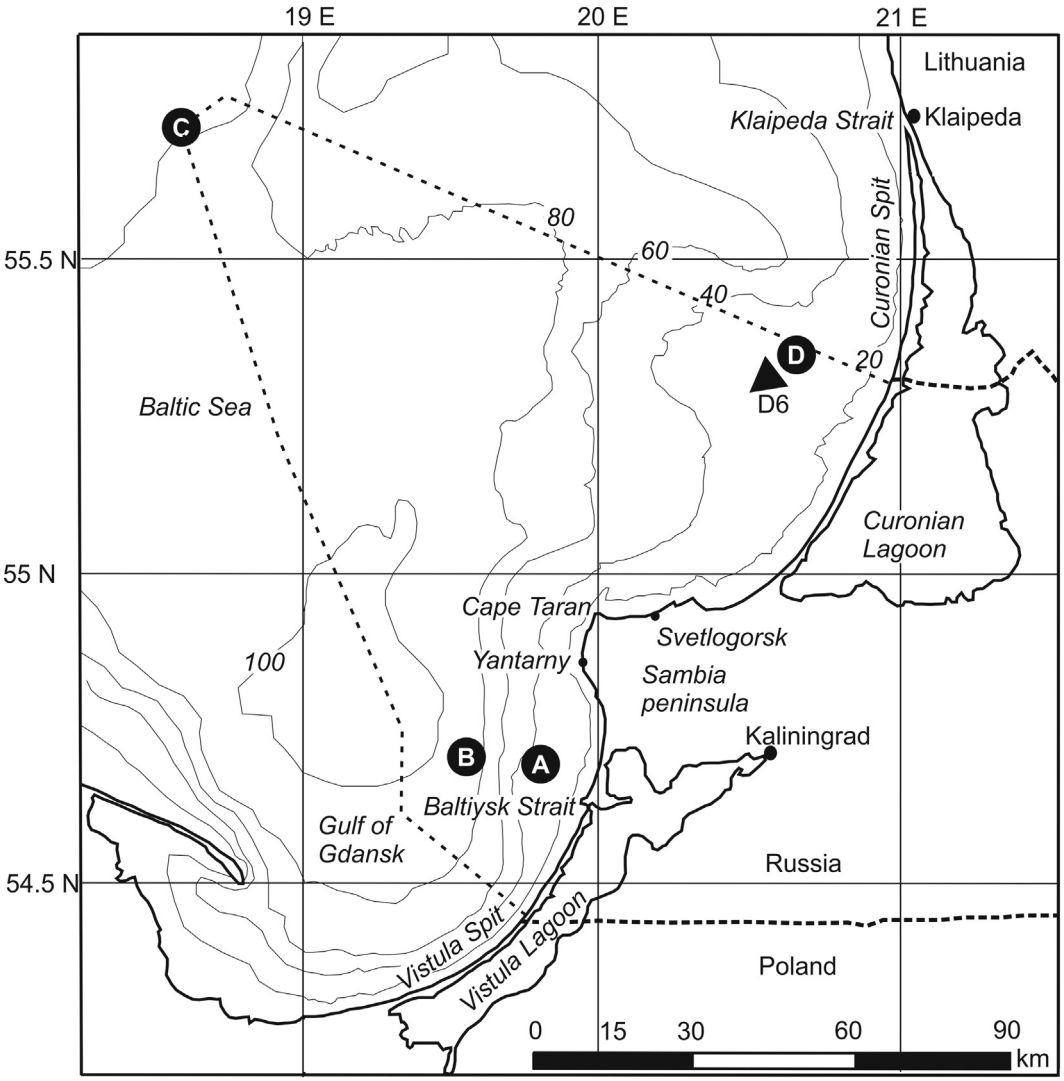

Fig. 3. Four stations in the southeastern part of the Baltic Sea within the Russian exclusive economic zone.

Table 1
Sampling stations, layers and weather conditions during sampling.

Station	Latitude	Longitude	Depth, m	WMO sea state, grade	Wind speed, m/s	Sampled layers, N	Layers description
A	54°43′37.2″	19°44′20.6″	30	1	4	4	Subsurface; in termo/halocline; between the thermocline and the bottom; above the bottom
B	54°45′15.3″	19°31′29.5″	93	1	0.1	5	Subsurface; in the thermocline; between the termo and the halocline; above the halocline; above the bottom
C	55°52′08.8″	18°57′46.1″	106	2	8	6	Subsurface; above the thermocline; CIL; above the halocline; between the halocline and the bottom; above the bottom (local salinity/temperature jump)
D	55°21′04.5″	20°40′04.9″	30	2	7	4	Subsurface; above the thermocline/halocline; between the halocline and the bottom; above the bottom

4. PLEX application and results

4.1. PLEX sampler

现场操作分工

At least two people were required to operate the PLEX. The first one operated the winch and water pump, controlled basic sampling parameters: penetration depth and volume of pumped water. The second one operated hoses, which required to be extracted manually from water, connected and disconnected the external vessel's water supply, washed hoses before sampling and replaced sample filters.

Pumping rate varied with sampling depth: it was 5 l/s in surface layers and decreased down to 2.8 l/s at the maximum sampling depth (91 m). Consequently, the time required to obtain the representative sample volume (2–3 m^3) varied from 7 to 18 min. The ship's time turned to be the most critical factor for sampling with PLEX. In order to established optimal sampling volume per ship's time spent, the volume of water pumped on different stations was slightly varied. The water volume was 3.3–3.5 m^3 per sample on A and B station, and was reduced down to 2.5 m^3 on C and D stations. The ship's time required to sample one station was directly proportional to sampling layers quantity and varied from 70 min on shallow stations up to 130 min on deep-water stations. However, we were able to combine sampling with the PLEX, deployed on the ship's stern, with other sampling activities that were conducted from the ship's bow. While sampling with PLEX was planned only on complex stations, the additional time required for sampling did not exceed one hour even on deep-water stations.

复杂的

Relatively calm weather conditions accompanied the sampling activities (Table 1). The observed sea state did not influence significantly the sampling procedure and, in general, amplitude of intake gauze penetration did not exceed 1 m. However, rougher sea state could increase amplitude significantly and coarsen the sampling results. Deployment of the PLEX sampling equipment on a ship's bow could also decrease accuracy of positioning of the intake gauze due to higher pitching.

During preliminary testing the system was deployed aboard a small research vessel NORD-3 (16 m in length), equipped with a power generator and an electric winch. The system operation requires at least 4 m^2 for deployment and operation plus additional area for a winch, a power generator and hoses. For coastal areas, where the depths do not exceed 30 m, the system can be deployed on the platform at least 4 × 4 m equipped with a manual winch and a moto pump or electric winch, electric pump and small moto generator (~3–5 kVA).

4.2. Quality control 质量控制

4.2.1. Blank samples 背景样本

Blanks from all the stations contained microplastics in form of fibers, films and paint flakes (Table 2). While fibers were present in all of the blanks, other forms of MPs were detected occasionally. Mean sample contamination was 8.3 ± 4.6 MP pcs/sample (CI, t-statistics, $p = 0.05$, $n = 4$) with fibers prevailing in numbers. Paint flakes found in blanks possibly originated from our research vessel. Thus, all paint flakes were excluded from further consideration. Fibers and films in blanks represented total airborne contamination which can originate both from the sampling activities on the ship's deck and laboratory analysis. However our previous study (Zobkov and Esiukova, 2017a),

油漆裂片

Table 2
Blank samples contamination.

Station	Fibers	Films	Fragments	Paint flakes	All forms
A	5	0	0	4	9
B	10	2	0	0	12
C	6	0	0	0	6
D	4	0	0	2	6

conducted in the same laboratory conditions, assessed the rate of laboratory contamination to be 0.5 fibers/sample only. Thus external sample contamination in the present study should have come mostly from the air on the ship's deck.

Relatively large seawater volume (2.5–3.3 m^3) collected with PLEX on every layer resulted in high MPs numbers detected in samples (in average 78.2 ± 47.9 MP pcs/sample, CI, t-statistics, $n = 19$). The difference between the MPs concentration in marine samples and blanks was statistically significant ($p = 0.0002 < 0.001$, Wilcoxon Signed Ranks Test). It enabled us to take the rate of contamination into account in the analytical results. The number of fibers and films found in blanks was subtracted from MPs numbers of the same form detected in every layer of the station, where these blanks were prepared. Films were not found in some of the samples or the numbers found were lower than the ones detected in blanks. In this case, the amount of this MPs form was set to zero. Raman spectra were successfully identified only for two films from blank samples. One green film was identified as polyethylene (PE) and for one blue flake synthetic due (SD) Cobalt Phthalocyanine was identified, however owing only a few number of specimens and their occasional identification in samples it is hard to establish their origin. Fibers found in blanks were too small to obtain Raman spectra.

4.2.2. Control samples

Control net washing samples were prepared only once per station and represent the sum of MPs numbers retained by the filter net on each station. This way of control was chosen instead of washing after each sample because of urgent need to reduce ship time required for sampling.

Every net washing sample contained MPs in form of fibers (in average 70.4 ± 39.3 pcs/sample, CI, t-statistics, $n = 4$), films (7.6 ± 4.2 pcs/sample) and fragments (1.0 ± 0.7 pcs/sample). Taking into account the volume of the integral sample (10–15 m^3), it allowed us to assess the net retaining ability, which was 5.2 ± 2.9 pcs/m^3 for fibers, 0.6 ± 0.5 pcs/m^3 for films, and 0.10 ± 0.05 pcs/m^3 for fragments, which was lower than MPs content on most of stations. However, it needs to be noted that in relation to total MPs numbers in a sample (Table 3), the maximum relative retaining ability was observed on **C** station for fibers, which apparently was connected with sampling fault during sampling of the fourth layer (59 m depth), when the outlet valve was closed most of the pumping time due to mishandling. However, relative retaining ability was 23% in average, and thus allows us to suppose that further results are relevant. Considering the integral MPs content on the station, the MPs content in net washing was added to the bulk mean calculated for separate layers.

The filtration unit was mounted horizontally during the sampling to prevent it from crushing during the ship pitching. In future, the net retaining ability can be reduced by the vertical repositioning of the filtration unit to let the gravity force make additional effort for net clearing. Subsequent straightening of the filtration unit holder will be required.

4.3. Vertical microplastic distribution

The **A** station was situated in the vicinity of the Strait of Baltiysk. Typically, warm and freshened plumes originating from the shallow

Table 3
The relative net retaining ability (MPs numbers retained by the net/total MPs numbers found on a station 100%).

Station	Fibers	Films	Fragments	All forms
A	13	10	0	12
B	22	10	14	20
C	45	25	11	40
D	17	34	20	19

and rapidly warming Vistula Lagoon evidently drift ashore and alongshore in this area (Lavrova et al., 2014). We observed the similar situation: vertical T-S structure (Fig. 4, station **A**) showed vertical advection of warmer and freshened water in the upper 3-m layer. Horizontal distribution of the salinity in the upper layer (Fig. 5) obtained by the data of CTD profiling showed that freshened waters from the Strait of Baltiysk moved long-shore in northern direction, and on station **A** the seaside margin of these waters was sampled for MPs content (Fig. 5).

Strong vertical stratification of MPs concentration with the highest fibers content in subsurface and intermediate layers was observed on the station. Such distribution can be explained by the presence of microplastics in freshened waters of the Strait of Baltiysk, which receives drainage from the Vistula River basin, Kaliningrad and populated regions of the Vistula Lagoon (Zobkov and Esiukova, 2017a). Fibers were dominant in subsurface layer; they were especially numerous at 6.9 m and their concentration linearly decreased with depth. This distribution is similar to the thermohaline structure. Probably, the corresponding water density gradient (pycnocline) hampers and prohibits the MPs sedimentation (Yurkovskis, 2005; Emeis et al., 2002; Pempkowiak et al., 2002).

Fragments content was the smallest on station A compared with other stations. It changed from 0.6 pcs/m^3 in the subsurface layer down to 0 pcs/m^3 above the bottom with a decrease in pycnocline and slight increase in the intermediate layer. Concentration of films was of the same order of magnitude as the one observed on other stations. Vertical variations of film concentrations were similar to those of fragments, but the observed films content was one order of magnitude higher than that of fragments (Fig. 4, station **A**).

Salinity gradient was not observed in the subsurface layer of station **B** and impact of warm and freshened waters from the Strait of Baltiysk cannot be recognized here. However, surface waters heated during the previous warming (Supplementary, Fig.S1) formed a weak seasonal (spring) thermocline in the layer at a depth of 11–16 m. The two-layer salinity stratification typical of the Baltic Sea is clearly seen: a freshened upper layer and a more saline deep layer are separated by the pycnocline (Chubarenko et al., 2017) at the depth of 60–65 m. The bottom layer of warmer and saline water with the thickness of up to 10 m was found at the depths of 80–90 m (Fig. 4, station **B**).

Fibers dominated over other forms of MP. Higher fibers content was observed in the subsurface and near bottom layers, while in the seasonal thermocline fibers content was the lowest on this station and increased stepwise with depth in the intermediate and pycnocline layers. Fragments stratification had the opposite structure: no fragments were found in the subsurface layer, while their maximum content was observed in the seasonal thermocline and it slightly decreased with depth down to zero in the pycnocline and slightly increased over the bottom. Films stratification showed intermediate character between fragments and fibers: the highest films content was observed in the subsurface layer and linearly decreased with depth down to the intermediate layer with an uptick in the pycnocline and sequential decrease over the bottom (Fig. 4, station **B**).

Salinity gradient was not observed in the upper layer of station **C**. Surface waters heated up to 4.3 °C and formed a weak thermocline at the depth of 11–15 m with a quasi-homogeneous upper 10-m layer (Fig. 4, station **C**). The thermohalocline formed during previous wintertime mixing was located at 55–64 m deep, while gradual temperature increase in overlying waters indicated the formation of the cold intermediate layer (CIL) (Chubarenko et al., 2017). The main halocline was formed at 58–63 m deep and the 8-m thick layer of warmer and saline waters was observed near the bottom.

Concentrations of films and fibers were relatively low in the subsurface layer comparing with **B** station, while the highest concentrations of these forms were observed over the seasonal thermocline (Fig. 4, station **C**).

The lowest content of all the forms was observed in the CIL with a

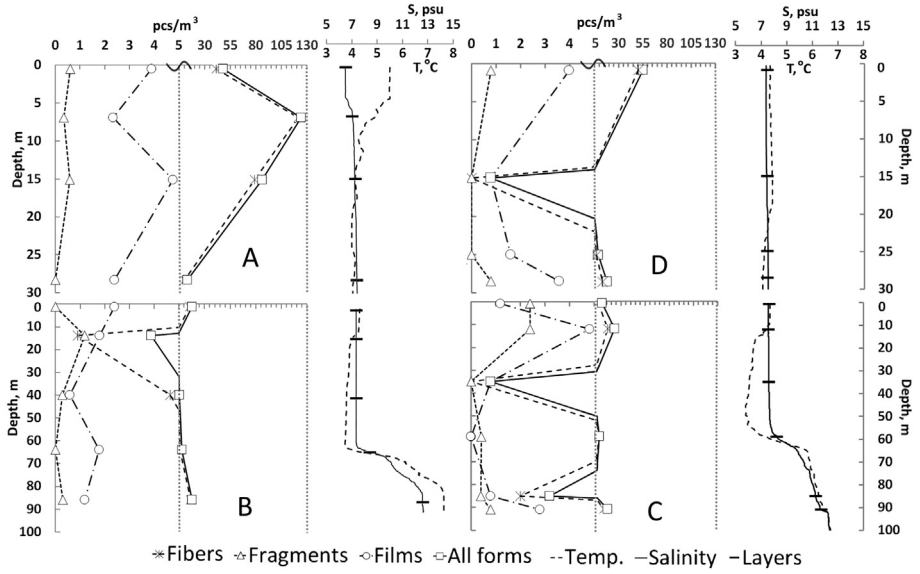

Fig. 4. Vertical distribution of concentrations of MPs forms (fibers, fragments, films) and the T,S structure on the sampled stations. Vertical density variations are defined by the water salinity, while influence of water temperature is minor. Note the change of the scale on the axis of MPs concentrations.

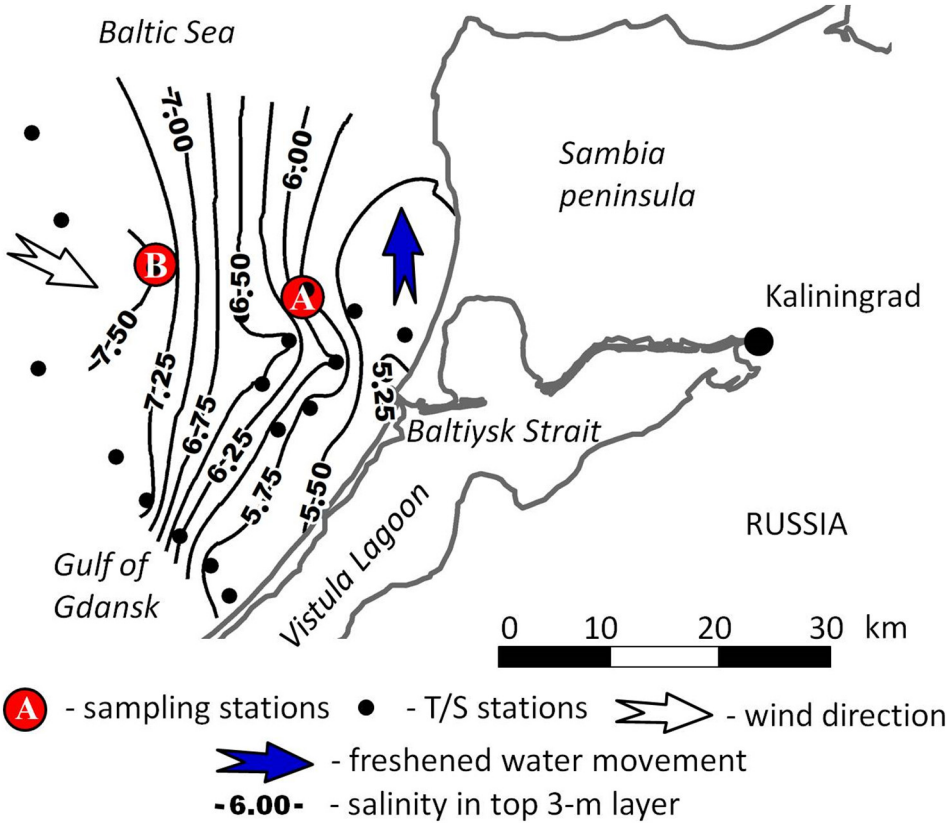

Fig. 5. Horizontal distribution of the mean salinity in the upper 3-m layer, obtained by CTD profiling in the area of the Strait of Baltiysk (03.04.17-04.04.17, cruise 135 r/v "Prof. Shtokman").

slight increase over the bottom and sharp spikes of fibers on temperature/salinity-induced density gradients.

Practically indistinguishable salinity gradient observed on station **D** indicates homogenous winter-time mixing over the coastal slope of the Curonian-Sambian plateau. A vertical temperature gradient formed during previous short warming episodes in March was perturbed by cold event with air temperatures down to 2.7 °C and winds of 7–11 m/s of northern directions during the sampling (Supplementary, Figs. S1, S2). It led to surface water layer cooling and intensive wind-wave mixing of earlier warmed surface waters (Fig. 4, station **D**).

Despite the intense wind-wave mixing, the highest MPs concentration was evident in a subsurface layer on the station with fibers prevailing above all other forms (Fig. 4, station **D**). The lowest MPs content was detected above the undeveloped halocline and it gradually increased with depth.

When all the stations are compared, it is clear that in coastal stations

扰乱

各观测点的对比

(**A** and **D**) fibers content in the upper layers was notably higher than on marine stations (**B**, **C**) (Fig. 4). Surprisingly, on the deeper layers, the content of all forms has the same order of magnitude at all the stations. The lowest MPs content was observed in the intermediate layers with an increase in the upper and near bottom layers, which fully coincides with previous observations in the Baltic Sea (Bagaev et al., 2017a, 2017b).

Since the MPs content on station A seemed to be influenced by the Strait of Baltiysk, it was excluded from the statistical analysis. The Mann-Whitney *U* test for **B**, **C** and **D** stations showed that the difference exists between MPs concentration in the intermediate layer and the subsurface layer ($p = 0.025 < 0.05$, Mann-Whitney *U* test, U = 0.0, z = 2.449), the intermediate layer and the thermohaline layer (*p*-value = 0.025 < 0.05, Mann-Whitney *U* test, U = 0.0, z = 2.236), the intermediate layer and the near bottom layer (*p*-value = 0.014 < 0.05, Mann-Whitney *U* test, U = 0.0, z = 2.449). Between the thermohaline, the near-bottom and the subsurface layers the differences were not statistically significant ($p \gg 0.05$, Mann-Whitney *U* test). Thus, these layers with elevated MPs content seem to be separated from each other by intermediate layers with low MPs content.

Colored microplastics sizes were distributed according to the log-normal law with size fractions < 1 mm prevailing in numbers, with the median MPs size of 0.95 mm. The Person *t*-test showed negative correlation between the logarithm of MP size and depth ($p = 1.67 \cdot 10^{-9} < 0.001$; $R = 0.315$; df = 348). Thus, MPs sizes seemed to decrease with depth according to the exponential low: $L = 1.48\ EXP(-0.01H)$, where L is the particle length, H – the sampling depth.

4.4. Mean MPs content

4.4.1. MPs abundance

The bulk mean content of MPs forms was calculated knowing MPs numbers in each sampled layer, the sampled layer thickness and overall depth (Table 4). MPs content in net washing samples was added to the calculated mean value to take into account the MPs retained by the filtering net.

4.4.2. Microplastics chemical composition

In total 122 microplastic specimens (mainly fibers, as the most abundant MPs type) were selected according to their morphological characteristics and 44 of them were successfully identified using μRaman spectroscopy. In other cases the identification was not possible due to small specimen size or strong background fluorescence. The same difficulties using μRaman spectroscopy in MPs identification were observed and discussed earlier (Ghosal et al., 2018). Between the successfully detected specimens 33 were identified as plastics of different types (Fig. 6): polyethylene terephthalate (PET), polyamide (Nylon, PA), polyethylene (PE), polypropylene (PP), polystyrene (PS), polyvinylchloride (PVC), polymethyl methacrylate (PMMA), and phenolic (PF) and polyterpene resins (PTR). One fiber was detected as pure carbon; however, it was equally thick, not tapering towards the ends, had a three-dimensional bending and clear and homogeneous violet color indicating its anthropogenic origin (Norén, 2007). Using μRaman spectroscopy carbon spectra could be obtained from the β-polyvinylidene fluoride (β-PVDF, fluorocarbon) polymer because of photochemical breakup of C—F bonds by laser irradiation (Ji et al., 2008). Knowing the morphological characteristic of the fiber, it was deemed to be a PVDF polymer. Three fibers were cellulose (CE), one was cellulose acetate (CA) and one was recognized as technical carbon (t-carbon) applied in wheel tires. These substances are not really plastics, however are man-made fibers and can be classified as marine litter. The core polymer type of five specimens was impossible to identify because the strong signal induced by synthetic dues (SD). Horasol Green G-K due was identified in two green fragments, Cobalt Phthalocyanine in one blue flake, Methylene Blue in a transparent light-blue fiber and Drimaten Turquose X-2G in one light-blue fiber. Considering all dues are of synthetic origin and usually applied as colorants for plastics, all such specimens were accounted as microplastics.

Polyvinyl methyl ether (PVME) was detected in three cases, once in a transparent fragment and twice in fibers (transparent and green-transparent). Under natural conditions PVME is not a solid polymer itself, but it can be applied in adhesives, release and surface coatings, lubricants, greases, elastomers, anticorrosion agents, molding compounds, personal care products, fiber and textile finishes (Polymer Properties Database. Polyvinyl ethers (PVE), 2015). Earlier it was found in cosmetics and household chemicals and was classified as “Unverified polymeric ingredient” (Fauna and Flora International, 2017). To our knowledge, this is the first observation of this polymer type in the marine environment, however owing to the polymer nature of this compound it was considered to be microplastics.

5. Discussion

The MPs content in blank samples was mainly induced by airborne contamination on the ship's deck. However, the fibers numbers in controls was not statistically significant compared with MPs concentration found in samples and the rate of background contamination was accounted in the results. The reduction of possible sources of contamination on the ship's deck during future sampling activities is possible by using polymers-free wear and instruments not only by the group working with MPs but also by all participants of the field survey.

The studies dealing with vertical profiles of MPs distribution or at least bulk water content are very scarce, which hampers comparison of the results. Moreover, they employ different sampling tools with different mesh sizes and different laboratory sample procession protocols, making quantitative comparison difficult (Hidalgo-Ruz et al., 2012). For example, the study conducted in the Gulf of Finland (the Baltic Sea) using the submersible pump for water sampling in subsurface layers with similar but smaller than ours mesh size (100 μm) reported only 0–6.8 MPs pcs/m^3 (Setälä et al., 2016). Offshore the Swedish eastern coast, (Gorokhova, 2015) using 90 μm WP2 nets reported at least three orders of magnitude higher concentrations (100–7.5 × 10^3 MPs pcs/m^3). High spatial variability, indicated by the standard deviation (SD) of almost the same value as the mean, also hampers data comparison with most of studies. However, qualitative variations of spatial and vertical MPs distribution can be compared.

Vertical MPs heterogeneity observed by (Gorokhova, 2015) in the upper 100-m layer of the Landsort Deep (459 m) in the Baltic Sea revealed not just vertical MPs structure heterogeneity, but also its seasonal variations. In summer on the depth of 30–60 m, which aligns with typical for the Baltic Sea halocline position in deep water regions (Leppäranta and Myrberg, 2009), MPs content was several orders higher than in the upper layer (0–30 m) and in winter the opposite vertical structure was observed with prevailing MPs content in the upper 30-m layer.

Previous studies of microliter in the Baltic Sea proper, conducted by our group using Niskin bottle samplers and the same mesh size (174 μm) (Bagaev et al., 2017b) one year earlier, in spring 2016 in the Gdansk basin during 131 cruise of RV Professor Shtokman, showed the microliter content to be three times higher (bulk mean 92.3 pcs/m^3, SD

Table 4
The mean (by volume) MPs content (pcs/m^3) on the sampled stations.

Station	Fibers	Films	Fragments	All forms
A	74.1	3.7	0.4	79.1
B	9.1	1.5	0.4	11.1
C	12.4	2.0	0.9	15.4
D	19.3	3.3	0.4	23.0
Mean	28.8	2.7	0.5	32.2
SD	48.6	1.7	0.4	50.4

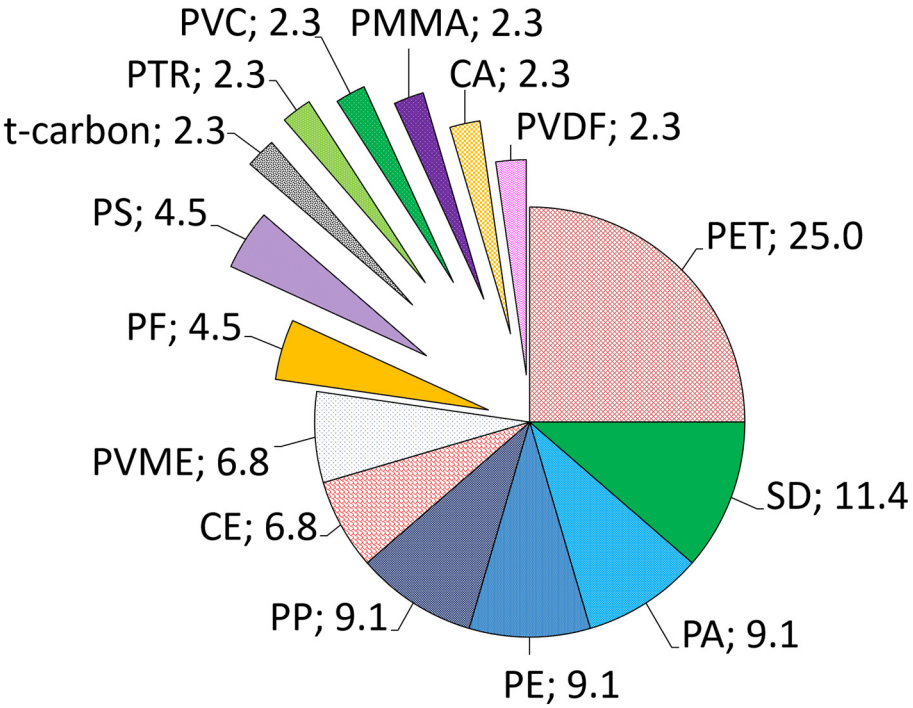

Fig. 6. Chemical composition of MPs specimens as percent (%) from the successfully identified with the μRaman spectroscopy.

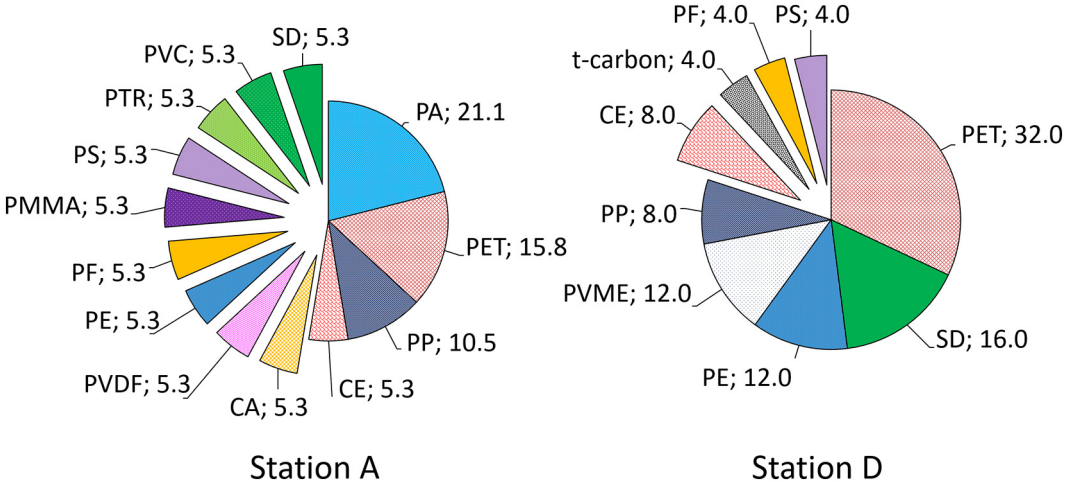

Fig. 7. Abundance of different polymer types (%) on stations A and D.

123 pcs/m^3) than presented here. However, if we exclude paint flakes (bulk mean 53.8 pcs/m^3), we will obtain mean content of 38.5 pcs/m^3, which is very close to the observed here (32.2 pcs/m^3). The pioneer water column studies conducted in the stratified Baltic Sea (Bagaev et al., 2017b) showed that MPs content at intermediate depths was 3–6 times lower than in the near-surface and near-bottom layers, with maximum in surface layers. Moore et al. (2005) also observed vertical MPs stratification in coastal waters off California, where maximum MPs numbers were found near the surface, lower contents - in intermediate layers; over the bottom they were higher than in intermediate, but smaller than in surface layers. On three (**B**, **C**, **D**) of four sites studied in the present work, the same distribution was observed and confirmed previous assumptions (Bagaev et al., 2017b). In the present study this heterogeneity is coupled with vertical thermohaline water structure and confirmed by the statistically significant difference between the MPs content in thermohaline, near-bottom, subsurface layers and intermediate layers.

The presence of high MPs content in coastal waters, and particularly fibers near the Strait of Baltiysk, is in good agreement with the study of Desforges et al. (2014) conducted at the northeast part of the Pacific Ocean, where fibers content in nearshore waters was statistically higher than in offshore waters, indicating terrestrial origin of fibrous MPs. The Strait of Baltiysk receives discharge from terrestrial territories with a population of more than one million people and many WWTP, including the city of Kaliningrad, discharges into the Vistula River and the Vistula Lagoon. The freshened water plumy located in the surface water layer on station **A** contained high fiber content, indicating their terrestrial origin. However, above the bottom the fibers content was of the same order of magnitude as on other stations (Fig. 4). This fact supports the idea that fibers in the upper and intermediate layers can originate from urbanized areas (Bagaev et al., 2017a), while fibers in near bottom layers come from deeper open sea areas along with the horizontal advection of cold saline waters (Cieślikiewicz et al., 2017; Myrberg and Andrejev, 2003; Babakov, 2010).

The domestic washings machines discharges were recently highlighted among other fibrous MPs sources (Browne et al., 2011) and the

high fiber numbers observed in surface and intermediate layers near the Strait of Baltiysk could definitely originate from this source. The chemical composition of fibrous MPs on station **A** (Fig. 7 station A) also supports this assumption: it can be seen that MPs found on this station mostly consisted of polyamide (PA), nylon (PET), polypropylene (PP), and cellulose (CE) (> 52% in total), which are frequently applied in textile industry and clothes production. The broad range of identified polymers (13) also indicates multifaceted MPs sources. This distribution is completely differed from the one observed on station **D** (Fig. 7, station D), where MPs were mainly presented by PET, PWME, PE, and PP fibers with only nine types of polymers identified. The Lukoil's Kravtsovskoye (D6) Oil Platform situated nearby the sampling site employs zero discharge principle and there are no other possible point sources of MPs near station D. However general fiber sources are poorly explored up to date (Cesa et al., 2017) and geotextiles are recently suggested as one of the possible sources of fibrous MPs (Wiewel and Lamoree, 2016; Cesa et al., 2017).

Geotextiles were seen to be widespread along the Sambia Peninsula shore from the Cape Taran to the root of the Curonian Spit (personal observations of Elena Esiukova from coastal surveys). Geosynthetics were applied in coastal protection structures, gabions, in construction of embankments to control erosion. Large sheets of geotextiles (geocells, woven and non-woven geotextiles) with traces of strong degradation seemed to have been torn away by storm actions and carried over long distances along the coastline (Fig. S3 in Supplementary). From 17 geotextiles specimens sampled during the coastal surveys on the Sambia Peninsula, 41% were proved to be PP followed by PET (35%), PE (11%), and PA (6%) using μRaman spectroscopy. Three from eight PET fibers successfully detected on station **D** (Fig. 8) showed Raman spectra identical to those of Dornite (Shkundin and Ronzhin, 1992). The Dornite specimen was sampled from the base of the boulder skirting of the promenade which is currently under construction in the town of Svetlogorsk. The sheets of this particular material together with some others were observed in abundance over the Sambia Peninsula and the Curonian Spit shores during coastal surveys. This indicated that geotextiles used in coastal protection structures may definitely be considered as a source of fibrous MPs in seas and can sufficiently contribute into the total MPs content in the environment.

6. Conclusion

Fifteen different polymer types were identified using μRaman spectroscopy and 89% of identified specimens were microplastics. Based on field surveys and μRaman spectroscopy analysis geotextiles applied in the coastal engineering structures seem to be the source of fibers found in the marine environment.

The observed strong heterogeneity of MPs distribution in previous and our findings highlighted that MPs are not necessarily concentrated near the surface, but may have comprehensive vertical structure in a stratified water column. The new PLEX sampler presented here showed its efficiency for coastal waters when collecting representative volumes of bulk water for quantitative MPs estimates down to 100 m deep. In the present design PLEX is unable to sample from the surface water layer, however for this purpose bulk water sampling with PLEX can be complemented with regular sampling activities with surface net towing. Application of specialized devices designed for this purpose is also possible. For example, real surface micro layer (SML) can be sampled using a 'meshing' technique (Song et al., 2014) or a rotating SML drum sampler (Carlson et al., 1988; Ng and Obbard, 2006). In future, to unify the sampling technology and achieve the best results using the unified contamination control method between surface and bulk water sampling techniques, the inlet gauze of the PLEX sampler can be set in a floating container to sample the surface water layer, however additional engineering efforts are required to avoid air inflow into the pumping system.

In the Baltic Sea, the vertical thermohaline structure plays a key role in vertical distribution of organic and inorganic particulate matter (Bełdowski et al., 2012; Lund-Hansen and Skyum, 1992; Bradtke and Krężel, 1994). Microplastics represent the same particulate matter with certain physical characteristics (size, shape, density, roughness etc.). They can be redistributed in the subsurface water layer with wind actions (Kukulka et al., 2012; Reisser et al., 2015). However, the vertical thermohaline water structure apparently acts as the sink buffer for microplastics. Temperature and salinity gradients are thus able to play a drastic role in MPs transport and retention in water column.

As it is known (Wyrtki, 1961; Wunsch, 2002; Rahmstorf, 2003), temperature and salinity stratification in the World Ocean provides driving forces for the slow but global thermohaline circulation. Polar water transport in deep water layers from the poles to the equator, the system of surface currents (the Gulf Stream, the Kuroshio etc.), deep ocean backflows, upwelling, downwelling and other processes all are natural forces caused by the vertical World Ocean stratification. Supporting the physical principles of vertical MPs distribution highlighted here, the vertical thermohaline structure of the World Ocean might be

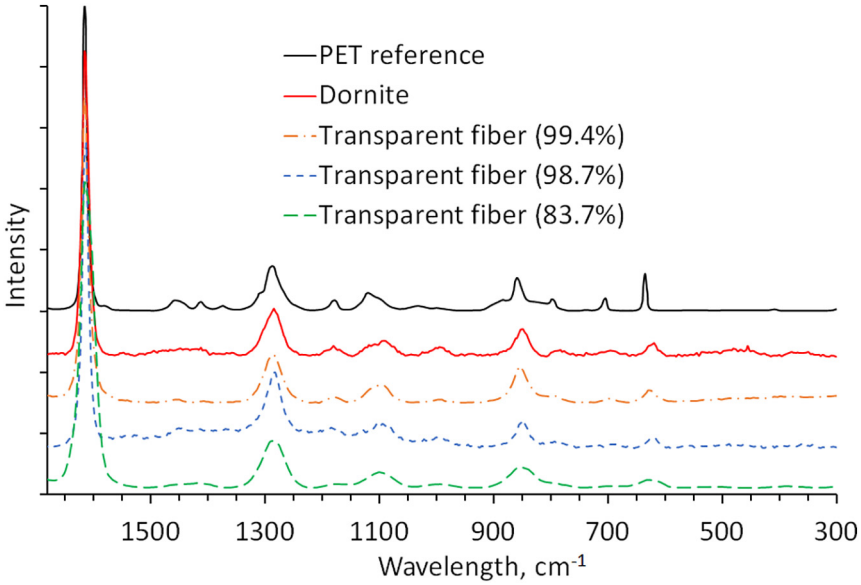

Fig. 8. Raman specters of fibers from station D, Dornite specimen, reference PET spectra and the hit ratio of fibers spectra to the ones of Dornite.

an unaccounted envelop for microplastics.
信封，遮盖

Acknowledgements

The investigations are supported by RFBR via grant number 18-55-76002 (ERA.Net RUS Plus S&T project 212 EI-GEO).

The field work was supported by the Russian Science Foundation via grant number 15-17-10020. Sample processing was performed in the Laboratory for Marine Physics under the state assignment № 0149-2018-0012.

The authors are especially grateful to Aleksei Grave for assistance in PLEX construction and infield operation.

Appendix A. Supplementary data

Supplementary data to this article can be found online at https://doi.org/10.1016/j.marpolbul.2018.11.047.

References

Andrady, A.L., 2011. Microplastics in the marine environment. Mar. Pollut. Bull. 62, 1596–1605. https://doi.org/10.1016/j.marpolbul.2011.05.030.

Araujo, C.F., Nolasco, M.M., Ribeiro, A.M., Ribeiro-Claro, P.J., 2018. Identification of microplastics using Raman spectroscopy: latest developments and future prospects. Water Res. 142, 426–440. https://doi.org/10.1016/j.watres.2018.05.060.

Babakov, A., 2010. Wind-driven currents and their impact on the morpho-lithology at the eastern shore of the Gulf of Gdańsk. Arch. Hydro-Eng. Environ. Mech. 57 (2), 85–104. Available at. http://www.ibwpan.gda.pl/docs/ahem/ahem57str085.pdf.

Bagaev, A., Mizyuk, A., Khatmullina, L., Isachenko, I., Chubarenko, I., 2017a. Anthropogenic fibres in the Baltic Sea water column: field data, laboratory and numerical testing of their motion. Sci. Total Environ. 599–600, 560–571. https://doi.org/10.1016/j.scitotenv.2017.04.185.

Bagaev, A., Khatmullina, L., Chubarenko, I., 2017b. Anthropogenic microlitter in the Baltic Sea water column. Mar. Pollut. Bull. https://doi.org/10.1016/j.marpolbul.2017.10.049.

Bełdowski, J., Bełdowska, M., Kuliński, K., Darecki, M., 2012. Vertical mercury, cadmium and lead distribution at two stratified stations in the Southern Baltic Sea. In: Nriagu, J., Market, B., Stavenga, M. (Eds.), Heavy Metals in the Environment. Maralte Books, pp. 237–256.

Bradtke, M., Krężel, A., 1994. Inhomogeneity of vertical distributions of suspended matter in the sea – consequences for remote sensing. Oceanologia 36 (1), 47–79. Available at. http://www.iopan.gda.pl/oceanologia/OC_36/OC36_1-4_Bradtke.pdf.

Browne, M.A., Crump, P., Niven, S.J., Teuten, E.L., Tonkin, A., Galloway, T., Thompson, R.C., 2011. Accumulations of microplastic on shorelines worldwide: sources and sinks. Environ. Sci. Technol. 45, 9175–9179. https://doi.org/10.1021/es201811s.

Carlson, D.J., Cantey, J.L., Cullen, J.J., 1988. Description of and result from a new surface microlayer sampling device. Deep-Sea Res. 35, 1205–1213. https://doi.org/10.1016/0198-0149(88)90011-8.

Carpenter, E.J., Smith, K.L., 1972. Plastics on the Sargasso Sea surface. Science 175 (4027), 1240–1241. https://doi.org/10.1126/science.175.4027.1240.

Cesa, F.S., Turra, A., Baruque-Ramos, J., 2017. Synthetic fibers as microplastics in the marine environment: a review from textile perspective with a focus on domestic washings. Sci. Total Environ. 598, 1116–1129. https://doi.org/10.1016/j.scitotenv.2017.04.172.

Checkley Jr., D.M., Ortner, P.B., Settle, L.R., Cummings, S.R., 1997. A continuous, underway fish egg sampler. Fish. Oceanogr. 6, 58–73. https://doi.org/10.1046/j.1365-2419.1997.00030.x.

Chubarenko, B., 2008. The Vistula lagoon. In: Chubarenko, B. (Ed.), Transboundary Waters and Basins in the South-East Baltic. 978-5-98777-031-3, pp. 37–57 Kaliningrad, Terra Baltica. (INTERNET resource).

Chubarenko, I., Bagaev, A., Zobkov, M., Esiukova, E., 2016. On some physical and dynamical properties of microplastic particles in marine environment. Mar. Pollut. Bull. 108, 105–112. https://doi.org/10.1016/j.marpolbul.2016.04.048.

Chubarenko, I., Demchenko, N., Esiukova, E., Lobchyk, O., Karmanov, K., Pilipchyk, V., Isachenko, I., Kyleshov, A., Tchygaevich, V., Stepanova, N., Krechik, V., Bagaiev, A., 2017. The formation of spring thermocline in the coastal zone of south-eastern Baltic Sea based on field data of 2010–2013. Oceanology 57, 632–638. https://doi.org/10.1134/S000143701705006X.

Cieślikiewicz, W., Dudkowska, A., Gic-Grusza, G., Jędrasik, J., 2017. Extreme bottom velocities induced by wind wave and currents in the Gulf of Gdańsk. Ocean Dyn. 67 (11), 1461–1480. https://doi.org/10.1007/s10236-017-1098-4.

Collignon, A., Hecq, J.H., Glagani, F., Voisin, P., Collard, F., Goffart, A., 2012. Neustonic microplastic and zooplankton in the North Western Mediterranean Sea. Mar. Pollut. Bull. 64 (4), 861–864. https://doi.org/10.1016/j.marpolbul.2012.01.011.

Cózar, A., Echevarría, F., González-Gordillo, J.I., Irigoien, X., Úbeda, B., Hernández-León, S., Palmae, Á.T., Navarrof, S., García-de-Lomasa, J., Ruizg, A., Fernández-de-Puellesh, M.L., Duarte, C.M., 2014. Plastic debris in the open ocean. Proc. Natl. Acad. Sci. U. S. A. 111 (28), 10239–10244. https://doi.org/10.1073/pnas.1314705111.

Desforges, J.P.W., Galbraith, M., Dangerfield, N., Ross, P.S., 2014. Widespread distribution of microplastics in subsurface seawater in the NE Pacific Ocean. Mar. Pollut. Bull. 79 (1–2), 94–99. https://doi.org/10.1016/j.marpolbul.2013.12.035.

Doyle, M.J., Watson, W., Bowlin, N.M., Sheavly, S.B., 2011. Plastic particles in coastal pelagic ecosystems of the Northeast Pacific ocean. Mar. Environ. Res. 71 (1), 41–52. https://doi.org/10.1016/j.marenvres.2010.10.001.

Emeis, K., Christiansen, C., Edelvang, K., Jähmlich, S., Kozuch, J., Laima, M., Leipe, T., Löffler, A., Lund-Hansen, L.C., Miltner, A., Pazdro, K., Pempkowiak, J., Pollehne, F., Shimmield, T., Voss, M., Witt, G., 2002. Material transport from the near shore to the basinal environment in the southern Baltic Sea. II: synthesis of data on origin and properties of material. J. Mar. Syst. 35, 151–168. https://doi.org/10.1016/S0924-7963(02)00127-6.

Enders, K., Lenz, R., Stedmon, C.A., Nielsen, T.G., 2015. Abundance, size and polymer composition of marine microplastics ≥ 10 μm in the Atlantic Ocean and their modelled vertical distribution. Mar. Pollut. Bull. 100 (1), 70–81. https://doi.org/10.1016/j.marpolbul.2015.09.027.

Eriksen, M., Lebreton, L.C.M., Carson, H.S., Thiel, M., Moore, C.J., Borerro, J.C., Galgani, F.G., Ryan, P.G., Reisser, J.W., 2014. Plastic pollution in the world's oceans: more than 5 trillion plastic pieces weighing over 250,000 tons afloat at sea. PLoS One 9 (12), e111913. https://doi.org/10.1371/journal.pone.0111913.

Fauna & Flora International, 2017. Removing or restricting microplastic ingredients or "microbeads" from consumer and industrial products. Guidance. Version 1. p. 48. Available at https://issuu.com/faunaflora/docs/microbeads-guidance-document.

Frias, J.P.G.L., Otero, V., Sobral, P., 2014. Evidence of microplastics in samples of zooplankton from Portuguese coastal waters. Mar. Environ. Res. 95, 89–95. https://doi.org/10.1016/j.marenvres.2014.01.001.

Ghosal, S., Chen, M., Wagner, J., Wang, Z.M., Wall, S., 2018. Molecular identification of polymers and anthropogenic particles extracted from oceanic water and fish stomach–a Raman micro-spectroscopy study. Environ. Pollut. 233, 1113–1124. https://doi.org/10.1016/j.envpol.2017.10.014.

Gorokhova, E., 2015. Screening for microplastic particles in plankton samples: how to integrate marine litter assessment into existing monitoring programs? Mar. Pollut. Bull. 99 (1–2), 271–275. https://doi.org/10.1016/j.marpolbul.2015.07.056.

Hidalgo-Ruz, V., Gutow, L., Thompson, R.C., Thiel, M., 2012. Microplastics in the marine environment: a review of the methods used for identification and quantification. Environ. Sci. Technol. 46 (6), 3060–3075. https://doi.org/10.1021/es2031505.

Jambeck, J.R., Geyer, R., Wilcox, C., Siegler, T.R., Perryman, M., Andrady, A., Narayan, R., Law, K.L., 2015. Plastic waste inputs from land into the ocean. Science 347 (6223), 768–771. https://doi.org/10.1126/science.1260352.

Ji, Y., Liu, J., Jiang, Y., Liu, Y., 2008. Analysis of Raman and infrared spectra of poly (vinylidene fluoride) irradiated by KrF excimer laser. Spectrochim. Acta A Mol. Biomol. Spectrosc. 70 (2), 297–300. https://doi.org/10.1016/j.saa.2007.07.061.

Khatmullina, L., Isachenko, I., 2017. Settling velocity of microplastic particles of regular shapes. Mar. Pollut. Bull. 114 (2), 871–880. https://doi.org/10.1016/j.marpolbul.2016.11.024.

Kukulka, T., Proskurowski, G., Morét-Ferguson, S., Meyer, D.W., Law, K.L., 2012. The effect of wind mixing on the vertical distribution of buoyant plastic debris. Geophys. Res. Lett. 39, L07601. https://doi.org/10.1029/2012GL051116.

Lattin, G.L., Moore, C.J., Zellers, A.F., Moore, S.L., Weisberg, S.B., 2004. A comparison of neustonic plastic and zooplankton at different depths near the southern California shore. Mar. Pollut. Bull. 49 (4), 291–294. https://doi.org/10.1016/j.marpolbul.2004.01.020.

Lavrova, O.Yu., Krayushkin, E.V., Solov'ev, D.M., Golenko, M.N., Golenko, N.N., Kalashnikova, N.A., Demidov, A.N., 2014. Influence of wind and hydrodynamic processes on propagation of the Vistula Lagoon waters into the Baltic Sea. In: Current Problems in Remote Sensing of the Earth From Space. 11(4). pp. 76–99 (in Russian).

Leppäranta, M., Myrberg, K., 2009. Physical Oceanography of the Baltic Sea. Springer, Praxis Publishing, Chichester, UK (370 pp).

Lund-Hansen, L.C., Skyum, P., 1992. Changes in hydrography and suspended particulate matter during a barotropic forced inflow. Oceanol. Acta 15, 339–346.

Lusher, A.L., Burke, A., O'Connor, I., Officer, R., 2014. Microplastic pollution in the Northeast Atlantic Ocean: validated and opportunistic sampling. Mar. Pollut. Bull. 88 (1–2), 325–333. https://doi.org/10.1016/j.marpolbul.2014.08.023.

Lusher, A.L., Tirelli, V., O'Connor, I., Officer, R., 2015. Microplastics in Arctic polar waters: the first reported values of particles in surface and sub-surface samples. Sci. Rep. 5, 14947. https://doi.org/10.1038/srep14947.

Masura, J., Baker, J., Foster, G., Arthur, C., 2015. Laboratory methods for the analysis of microplastics in the marine environment: recommendations for quantifying synthetic particles in waters and sediments. In: NOAA Technical Memorandum NOS-OR&R-48, Available at. http://marinedebris.noaa.gov/sites/default/files/publications-files/noaa_microplastics_methods_manual.pdf.

Moore, C.J., Lattin, G.L., Zellers, A.F., 2005. Density of plastic particles found in zooplankton trawls from coastal waters of California to the North Pacific Central Gyre. In: The Plastic Debris Rivers to Sea Conference, Redondo Beach, California, USA.

Myrberg, K., Andrejev, O., 2003. Main upwelling regions in the Baltic Sea - a statistical analysis based on three-dimensional modelling. Boreal Environ. Res. 8, 97–112. Available at. http://www.borenv.net/BER/pdfs/ber8/ber8-097.pdf.

Ng, K.L., Obbard, J.P., 2006. Prevalence of microplastics in Singapore's coastal marine environment. Mar. Pollut. Bull. 52 (7), 761–767. https://doi.org/10.1016/j.marpolbul.2005.11.017.

Norén, F., 2007. Small plastic particles in coastal Swedish waters. In: KIMO Report, pp. 1–11. Available at. http://www.n-research.se/pdf/Small%20plastic%20particles%20in%20Swedish%20West%20Coast%20Waters.pdf.

Pempkowiak, J., Beldowski, J., Pazdro, K., Staniszewski, A., Leipe, T., Emeis, K.-C., 2002. The contribution of the fine sediment fraction to the fluffy layer suspended matter. Oceanologia 44 (4), 513–527. Available at. http://www.iopan.gda.pl/oceanologia/444pempk.pdf.

Polymer Properties Database. Polyvinyl ethers (PVE), 2015. Available at. https://

polymerdatabase.com/polymer%20classes/Polyvinylether%20type.html.
Rahmstorf, S., 2003. Thermohaline circulation: the current climate. Nature 421 (6924), 699. https://doi.org/10.1038/421699a.
Reisser, J., Slat, B., Noble, K., du Plessis, K., Epp, M., Proietti, M., de Sonneville, J., Becker, T., Pattiaratchi, C., 2015. The vertical distribution of buoyant plastics at sea: an observational study in the North Atlantic Gyre. Biogeosciences 12 (4), 1249. https://doi.org/10.5194/bg-12-1249-2015.
Rozynski, G., Bielecka, M., Margonski, P., Psuty, I., Szhymanek, L., Chubarenko, B., Esiukova, E., Domnin, D., Domnina, A., Pilipchuk, V., 2015. Chapter 7. The physio-geographical background and ecology of the Vistula Lagoon. In: Lillebo, A.I., Stalnacke, P., Gooch, G.D. (Eds.), Coastal Lagoons in Europe. IWA Publishing Alliance House, London, pp. 57–67.
Setälä, O., Magnusson, K., Lehtiniemi, M., Norén, F., 2016. Distribution and abundance of surface water microlitter in the Baltic Sea: a comparison of two sampling methods. Mar. Pollut. Bull. 110 (1), 177–183. https://doi.org/10.1016/j.marpolbul.2016.06.065.
Shkundin, B.M., Ronzhin, I.S., 1992. Geotextiles in water project construction. Hydrotech. Constr. 26 (4), 256–258. Available at. https://link.springer.com/content/pdf/10.1007/BF01545330.pdf.
Song, Y.K., Hong, S.H., Jang, M., Kang, J.-H., Kwon, O.Y., Han, G.M., Shim, W.J., 2014. Large accumulation of micro-sized synthetic polymer particles in the sea surface microlayer. Environ. Sci. Technol. 48 (16), 9014–9021. https://doi.org/10.1021/es501757s.
Tagg, A., Harrison, J.P., Ju-Nam, Y., Sapp, M., Bradley, E.L., Sinclair, C.J., Ojeda, J.J., 2017. Fenton's reagent for the rapid and efficient isolation of microplastics from wastewater. Chem. Commun. 53, 372–375. https://doi.org/10.1039/C6CC08798A.
Thompson, R.C., Olsen, Y., Mitchell, R.P., Davis, A., Rowland, S.J., John, A.W., McGonigle, D., Russell, A.E., 2004. Lost at sea: where is all the plastic? Science 304 (5672), 838. https://doi.org/10.1126/science.1094559.
Wiewel, B.V., Lamoree, M., 2016. Geotextile composition, application and ecotoxicology—A review. J. Hazard. Mater. 317, 640–655. https://doi.org/10.1016/j.jhazmat.2016.04.060.
Woodall, L.C., Sanchez-Vidal, A., Canals, M., Paterson, G.L.J., Coppock, R., Sleight, V., Calafat, A., Rogers, A.D., Narayanaswamy, B.E., Thompson, R.C., 2014. The deep sea is a major sink for microplastic debris. R. Soc. Open Sci. 1 (4), 140317. https://doi.org/10.1098/rsos.140317.
Wunsch, C., 2002. What is the thermohaline circulation? Science 298 (5596), 1179–1181. https://doi.org/10.1126/science.1079329.
Wyrtki, K., 1961. The thermohaline circulation in relation to the general circulation in the oceans. Deep-Sea Res. 8 (1), 39–64. https://doi.org/10.1016/0146-6313(61)90014-4.
Yurkovskis, A., 2005. Seasonal benthic nepheloid layer in the Gulf of Riga, Baltic Sea: sources, structure and geochemical interactions. Cont. Shelf Res. 25, 2182–2195. https://doi.org/10.1016/j.csr.2005.08.020.
Zhao, J., Lui, H., McLean, D.I., Zeng, H., 2007. Automated autofluorescence background subtraction algorithm for biomedical Raman spectroscopy. Appl. Spectrosc. 61 (11), 1225–1232. https://doi.org/10.1366/000370207782597003.
Zhao, S., Zhu, L., Wang, T., Li, D., 2014. Suspended microplastics in the surface water of the Yangtze Estuary System, China: first observations on occurrence, distribution. Mar. Pollut. Bull. 86 (1–2), 562–568. https://doi.org/10.1016/j.marpolbul.2014.06.032.
Zhao, S., Zhu, L., Li, D., 2015. Microplastic in three urban estuaries, China. Environ. Pollut. 206, 597–604. https://doi.org/10.1016/j.envpol.2015.08.027.
Zobkov, M., Esiukova, E., 2017a. Microplastics in Baltic bottom sediments: quantification procedures and first results. Mar. Pollut. Bull. 114, 724–732. https://doi.org/10.1016/j.marpolbul.2016.10.060.
Zobkov, M., Esiukova, E., 2017b. Evaluation of the Munich Plastic Sediment Separator efficiency in extraction of microplastics from natural marine bottom sediments. Limnol. Oceanogr. Methods 15, 967–978. https://doi.org/10.1002/lom3.10217.